

## Bjerrum pairing correlations at charged interfaces

A. TRAVESSET and D. VAKNIN

*Department of Physics and Astronomy and Ames Laboratory, Iowa State University  
Ames, IA, 50011, USA*

received 7 November 2005; accepted in final form 13 February 2006

published online 1 March 2006

PACS. 82.45.Mp – Thin layers, films, monolayers, membranes.

PACS. 61.20.Qg – Structure of associated liquids: electrolytes, molten salts, etc.

PACS. 82.39.Jn – Charge (electron, proton) transfer in biological systems.

**Abstract.** – Electrostatic correlations play a fundamental role in aqueous solutions. In this letter, we identify *transverse* and *lateral* correlations as two mutually exclusive regimes. We show that the transverse regime leads to binding by generalization of Bjerrum pair formation theory, yielding binding constants from first-principle statistical-mechanical calculations. We compare our theoretical predictions with experiments on charged membranes and Langmuir monolayers and find good agreement. We contrast our approach with existing theories in the strong-coupling limit and on charged modulated interfaces, and discuss different scenarios that lead to charge reversal and equal-sign attraction by macro-ions.

*Introduction.* – In recent years it has been recognized that the precise ion distribution next to charged macromolecules is a key problem for understanding biological processes such as cell signaling, membrane fusion or DNA replication and is also of fundamental relevance in many industrial applications. Ample theoretical and experimental efforts, reviewed in [1, 2], have been devoted to the problem.

The standard theoretical approach for describing ions in solution next to charged interfaces is the Poisson-Boltzmann (PB) theory. PB theory, however, ignores correlations, which are believed to play a fundamental role when the interfaces are strongly charged and the solution contains multi-valent ions. A new strong-coupling (SC) regime, defined by  $\Gamma \equiv a_C/\lambda_G \gg 1$ , where  $a_C$  is a typical counterion separation near the interface and  $\lambda_G$  is the Gouy-Chapman length, has been identified, and different SC theories have been proposed [3–6]. These theoretical descriptions usually assume that the charge at the interface is smeared to a uniform density, whereas realistic interfaces consist of discrete charges. Theoretical models incorporating the discreteness of interfacial charges have been introduced recently, both within SC [7, 8] and PB [9, 10].

Rather surprisingly, there are many experimental examples that show that PB theory combined with a Langmuir adsorption theory (LPB) [11], where ion adsorption to the interface is empirically included by binding constants, adequately describes divalent ion distributions, both near membranes [12] and Langmuir monolayers [13]. It has been shown, for example, that divalent ion distributions near fatty acid charged Langmuir monolayers ( $\Gamma \approx 20$ ) are

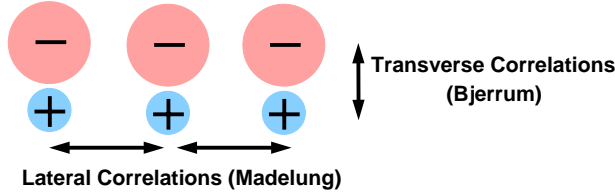


Fig. 1 – Schematic view of the transverse and lateral correlation regimes discussed in this paper.

described by LPB with a striking accuracy [13]. This result is somewhat unexpected, as it seems inescapable that tightly bound divalent ions to the interface are laterally correlated, which should result in an additional contribution to the LPB free energy (the Madelung energy) which is given by (see [14] and references therein)

$$F_{corr} \approx -2.101\sqrt{2}\frac{l_B}{a_L}k_B T \approx -4.2k_B T, \quad (1)$$

where  $l_B = 7.1 \text{ \AA}$  is the Bjerrum length and  $a_L \approx 4.8 \text{ \AA}$  is the lattice constant of a fatty acid in the crystalline phase. As shown below (see fig. 4), when the Madelung contribution eq. (1) is accounted for within LPB, the agreement between theory and experiment is completely ruined. In this letter, we consider *transverse* (as opposed to *lateral*) correlations (see fig. 1) between the counterions and the discrete interfacial charges and show that they induce binding by generalizing Bjerrum theory [15]. The free energy of the system becomes equivalent to LPB but now the binding constants are electrostatic in origin and can be computed explicitly.

The Bjerrum pairing theory establishes that opposite charged ions of valence  $q_+$  and  $q_-$  and radii  $r_+$  and  $r_-$  in bulk solution form pairs, with an association constant  $K_B$  (defined by  $K_B = [AB]/[A^+][B^-]$ , where  $[X]$  is the electrolyte concentration) given by [15]

$$K_B = 4\pi \int_d^{|q_+q_-|l_B/2} dr r^2 \exp(-q_+q_-l_B/r) = 4\pi(|q_+q_-|l_B)^3 G\left(\frac{|q_+q_-|l_B}{d}\right), \quad (2)$$

where  $d = r_+ + r_-$  and  $G(x) = \int_2^x dz z^{-4} e^z$ . We interpret Bjerrum pairing as implying that if two oppositely charged ions come closer than a distance  $D \leq \frac{|q_+q_-|\epsilon^2}{2\epsilon k_B T} \equiv |q_+q_-|l_B/2$ , they attract more strongly than the disordering thermal fluctuations and bind. First-principles expressions for Bjerrum constants [16] are numerically indistinguishable from eq. (2). Bjerrum theory has been recently emphasized in many contexts such as, for example, in Coulomb criticality [17].

*Correlations in the zero-temperature limit.* – In some electrostatic problems, insight into finite-temperature regimes can be obtained from the analysis of the zero-temperature limit [10,14,18]. As a simple model for quantitatively analyzing correlations, we consider the extreme case of  $N_P$  charged particles arranged as a two-dimensional (2D) triangular crystal, interacting with  $N_P$  oppositely charged particles arranged as another 2D triangular crystal, see fig. 2. Both crystals have the same lattice constant  $a_L$  and area of unit cell  $A_C$ . We compute the electrostatic energy as a function of the distance  $z$  between the two planes for two situations, where the lattices are either opposite or staggered to one another (see fig. 2). This calculation is performed exactly by Ewald summation techniques (see [14] and references therein). Figure 2 shows that the opposite configuration has lower electrostatic energy and we therefore analyze it in more detail.

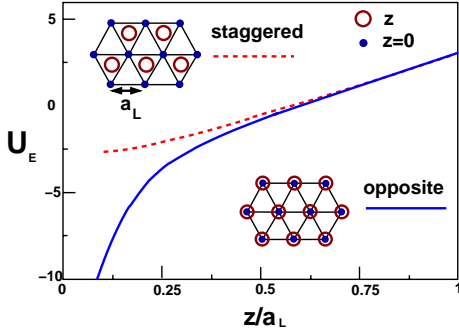


Fig. 2

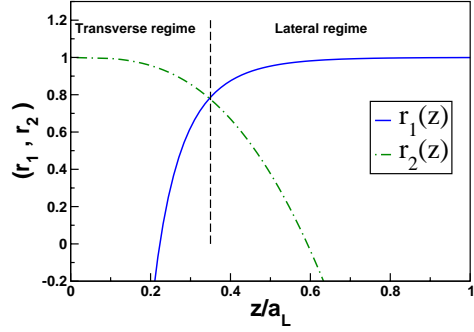


Fig. 3

Fig. 2 – Electrostatic energy  $U_E$  (in units of  $e^2q^2/\epsilon a_L$ ) as a function of separation for two triangular two-dimensional lattices of opposite charge (of equal valence  $q$ ) in both the opposite and staggered configuration.

Fig. 3 – Electrostatic energy parameterized by the two ratios defined in eq. (5) defining the interface and the ion-ion regimes for the opposite configuration.

As a function of the separation ( $z$ ), the electrostatic energy can be divided into two regimes. The transverse correlation (TC) regime ( $z \ll a_L$ ), where the energy is dominated by the attraction of close opposite sign charges,

$$U_S(z) = -N_P \frac{e^2}{\epsilon z}, \quad (3)$$

and the lateral correlation (LC) regime ( $z \gg a_L$ ), where the energy consists of the two Madelung energies  $U_M$  (one for each individual lattice) plus the energy of a planar capacitor with the smeared surface charge of the lattices and width  $z$ . More precisely,

$$U_L(z) = N_P \left( 2U_M + \frac{2\pi e^2 z}{\epsilon A_C} \right). \quad (4)$$

We characterize the two regimes (schematically shown in fig. 1) by defining two ratios measuring deviations of the electrostatic energy  $U_E(z)$  relative to their asymptotic values, eqs. (4) and (3),

$$r_1(z) = \frac{U_E(z) - 2N_P U_M}{\frac{2\pi e^2 z N_P}{A_C}}, \quad r_2(z) = \frac{U_E(z)}{U_S(z)}. \quad (5)$$

The transition separating the two regimes is sharp (fig. 3), defining a new characteristic length  $z_0 \sim 0.35a_L$  separating the TC and LC regimes. The length  $z_0$  is a property of the interface, independent of solution conditions (ionic strength, temperature, etc.).

*Bjerrum pairing induced correlations.* – We first discuss the simpler situation of a uniform charged interface with counter-ions of valence  $q$ . The first equation of the Yvon-Born-Green (YBG) hierarchy is an exact relation between the ion distribution  $n(z)$ , and the counterion-counterion pair distribution function  $g(\mathbf{r}, \mathbf{r}')$  [19],

$$-k_B T \frac{dn(z)}{dz} = -q \frac{2\pi\sigma}{\epsilon} n(z) + \int d^3\mathbf{r}' n(z) n(z') g(\mathbf{r}, \mathbf{r}') \frac{\partial V(|\mathbf{r} - \mathbf{r}'|)}{\partial z}, \quad (6)$$

TABLE I – Values in  $pK_I$  units ( $pK_I = \log_{10}(K_I)$ ) for the binding constants eq. (8) of different counterions to oxygen ( $r_- = 1.6 \text{ \AA}$ ). The bare (crystallographic) radius  $r_+$  of the ions is used except for  $\text{Mg}_H^{2+}$ , for which the hydrated radius is used. (Units of  $K_I$  are  $1 \text{ M}^{-1}$ .)

| Interface charge ( $q_I$ ) | $\text{Na}^+$ | $\text{K}^+$ | $\text{Cs}^+$ | $\text{Ca}^{2+}/\text{Cd}^{2+}$ | $\text{Ba}^{2+}$ | $\text{Mg}^{2+}$ | $\text{Mg}_H^{2+}$ | $\text{La}^{3+}$ |
|----------------------------|---------------|--------------|---------------|---------------------------------|------------------|------------------|--------------------|------------------|
| -1                         | -0.44         | -0.63        | -1.05         | +0.98                           | +0.90            | 1.10             | 0.23               | +1.869           |
| -2                         | +1.00         | +0.91        | +0.82         | +2.80                           | +2.53            | 3.22             | 1.80               | +4.965           |

where  $V(r) = q^2 e^2 / (\epsilon r)$ . If  $g(\mathbf{r}, \mathbf{r}') = 1$  (no correlations) the above equation is equivalent to PB. If, however, we assume a strong electrostatic repulsion where each ion excludes every other like-sign ion  $g(\mathbf{r}, \mathbf{r}') = 0$  then the calculated density profile is

$$n(z) = \frac{1}{2\pi l_B \lambda_G^2} \exp[-z/\lambda_G], \quad (7)$$

where  $\lambda_G$  is the Gouy-Chapman length. This result is the counter-ion density profile within SC [3,4]. The second equation in the YBG hierarchy can now be used to obtain the correction to  $g = 0$ , leading to  $g(\mathbf{r}, \mathbf{r}') = \exp\left[-\frac{q^2 l_B}{|\mathbf{r} - \mathbf{r}'|}\right]$ . This result establishes the range of validity for the approximation  $g \approx 0$  as defined by the condition  $|\mathbf{r} - \mathbf{r}'| \ll q^2 l_B$ .

We now consider discrete interfacial charges. If  $q_-$  is the valence of the discrete interfacial charges, the same steps as above give the counterion density  $n(\mathbf{r}) \propto \exp\left[\frac{|q_+ q_-| l_B}{|\mathbf{r} - \mathbf{r}'|}\right]$ , which is asymptotically exact for  $z \ll |q_+ q_-| l_B$ . Mobile ions “see” the interfacial charge as if no other charges are present in the system. From the Bjerrum argument outlined in the introduction, interface-ion pair-association then follows with a binding constant

$$K_I = \frac{K_B}{2}, \quad (8)$$

where  $K_B$  has been defined in eq. (2). The 1/2 prefactor in eq. (8) results from the fact that half of the space (let us say the  $z < 0$  region) becomes inaccessible to the mobile ions because of the presence of the rigid interface. Selected values for the constants, eq. (8), are given in table I.

*Free energy and counter-ion profiles.* – The free energy of the system consists of a “Stern” layer of bound ions induced by TC and a bulk solution containing the remaining unbound ions. If  $n_a^B$  is the bulk concentration of counterions of type  $a$ ,  $f_a$  the fraction of bound ions and  $K_L^a$  the association constant of ion  $a$  to the interfacial charged groups, the free energy is

$$\frac{F}{N_P k_B T} = - \sum_a f_a \ln(K_L^a n_a^B) + \left(1 - \sum_a f_a\right) \ln\left(1 - \sum_a f_a\right) + \sum_a f_a \ln(f_a) + \frac{F_{PB}(\sigma(f_a))}{N_P k_B T}. \quad (9)$$

The binding free energy gain for  $f_a N_P$  ions is  $-f_a N_P \ln(K_L^a)$  and the loss of entropy is  $-N_P f_a \ln(n_a^B)$ . These two contributions combine in the first term of the free energy. The next term is the mixing entropy of the interfacial species, and the last term  $F_{PB}$  is the free energy of the remaining unbound ions. We restrict the analysis to the dilute limit, where the activity coefficient of the ions may be approximated as unity, so  $F_{PB}$  is the PB free energy of a solution containing the remaining free (not bound) ions, thus keeping the number of free and bound ions constant. Minimization of the free energy with respect to  $f_a$  leads to

$$f_a = \frac{K_L^a n_a^B \exp[-q_a \phi(0)]}{1 + \sum_a K_L^a n_a^B \exp[-q_a \phi(0)]}. \quad (10)$$

TABLE II – Comparison between experimental and theoretical (eq. (8) and eq. (2))  $pK$  values. Carbonic (Carb.) and Phosphoric (Phos.)  $pK$  values are reported in [20] for single (–1) and double (–2) deprotonated acids.

| Ion              | $pK_I$ (membrane) |           |           | $pK_B$ (solution) |       |       |              |       |       |
|------------------|-------------------|-----------|-----------|-------------------|-------|-------|--------------|-------|-------|
|                  | Eq. (8)           | Exp. [21] | Exp. [22] | Eq. (2) (–1)      | Carb. | Phos. | Eq. (2) (–2) | Carb. | Phos. |
| Na <sup>+</sup>  | –0.44             | –0.6      | –0.35     | –0.14             |       |       | 0.90         |       |       |
| Ba <sup>2+</sup> | +0.90             |           |           | +1.2              |       |       | 2.83         | 2.83  |       |
| Ca <sup>2+</sup> | +0.98             | 1.0       |           | +1.3              | 1.0   | 1.4   | 3.1          | 3.15  | 2.74  |

The effective surface charge density is  $\sigma(f_a) = \sigma_0 \frac{-1 + \sum_a (q_a - 1) K_L^a n_a^B \exp[-q_a \phi(0)]}{1 + \sum_a K_L^a n_a^B \exp[-q_a \phi(0)]}$ , where  $\sigma_0 = -e/A_c$  and  $\phi(0)$  is the contact value potential in units of  $k_B T/e$ . It is assumed that counterions bind in a 1 : 1 ratio to the charges at the interface. It is trivial to include binding in a 2 : 1 (2 surface charges to 1 counterion) ratio, which may occur in some membranes [22].

From our previous discussion it should be expected that  $K_L^a$  is given by  $K_I^a$ , eq. (8). It should be noted, however, that  $K_I^a$  is obtained by integration of a half-sphere of radius  $|q_I q_a| l_B / 2$ , where the mobile ion “sees” the interfacial charge as the only charge in the system. From the discussion following fig. 3, however, the mobile ion can only “see” the interface charge if it is within a distance  $z_0 \sim 0.35 a_L$  from the interface. There are therefore two cases that need to be considered. If  $z_0 > |q_I q_a| l_B / 2$  the association constant is given by eq. (8), but if  $z_0 \ll |q_I q_a| l_B / 2$  the integration defining eq. (8) is restricted to a much smaller domain and the actual constant  $K_L$  is smaller than  $K_I$ ,

$$K_L^a = K_I^a \quad (a_L \geq \alpha |q_I q_a| l_B), \quad K_L^a \ll K_I^a \quad (a_L \ll \alpha |q_I q_a| l_B), \quad (11)$$

where  $\alpha \approx 1$ –1.4. In cases where the ion binding is covalent, the previous formulas do not apply. An important example is the proton, but the association constants for the proton follow from  $pK_a$  values ( $pK_a = 2.16$  and  $pK_a = 5.1$  for phosphate and carboxyl groups, respectively).

*Comparison with experiment.* – We selected three ions with the atomic structure of the noble gas: Na<sup>+</sup>, Ba<sup>2+</sup> and Ca<sup>2+</sup>, binding to carboxyl (–COOH) and phosphate (–PO<sub>4</sub>H) groups (in both cases, the binding is to an oxygen atom) and compared our predictions to available experimental results in table II. In order to assess the validity of using the bare radius for oxygen in eq. (8), we included binding constants to small soluble molecules containing the same groups, which are described by eq. (2). The agreement with experiment is satisfactory.

Fatty acids are strongly charged systems ( $\Gamma \approx 20$ ) and are appropriate for investigations of the SC limit. A first qualitative prediction of our approach is that divalent ions should form a tight “Stern” layer, with almost negligible distribution, next to the interface. This is well established experimentally from many X-ray reflectivity studies after the pioneering work by Kjaer *et al.* [23]. On a more quantitative level, we use the data on arachidic acid (AA) obtained by infrared reflection-absorption spectroscopy (IRRAS) [24].

Figure 4 shows IRRAS experimental results [24]. The solid line plots the degree of dissociation expected from the LPB free energy, eq. (9). We used the expected  $pK_a = 5.1$  of the carboxyl group and fitted the association constant to the experimental data. For calcium,  $pK = 0$  is obtained. This value is one order of magnitude smaller than the predicted value in table I, but this should be expected given eq. (10) and the fact that typical interfacial charge separation (the lattice constant for AA) satisfies  $a_L \approx 4.8 \text{ \AA} \ll 2l_B = 14.2 \text{ \AA}$ . For Cd<sup>2+</sup>  $pK = 1.8$  is obtained. This value seems in contradiction with table II and eq. (10). However, Cd<sup>2+</sup> ions do not have a noble-gas structure and covalent bonding with oxygen is possible.

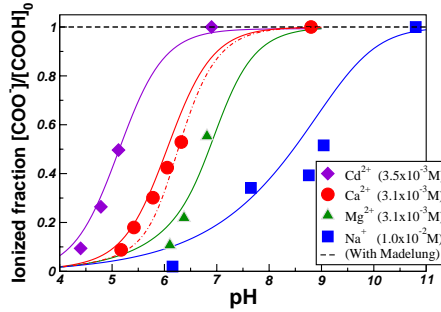


Fig. 4 – Dissociation of arachidic acid as a function of  $pH$ . The symbols are the experimental results from [24]. The solid lines are the results from eq. (9) with a 1 : 1 binding. The dash-dotted line corresponds to a 2 : 1 binding for calcium and the dashed line shows the result of including the Madelung term eq. (1) into the free energy eq. (9).

This has been confirmed from IRRAS data [25]. We should note that if the binding is indeed covalent, the  $pK$  value obtained should be identical with the critical stability constants [20]  $pK = 1.8$ , in agreement with our result. The constant for  $Mg^{2+}$  is  $pK \approx -1.4$ . Given that  $Mg^{2+}$  ion has a smaller radius than  $Ca^{2+}$ , eq. (8) predicts a stronger  $Mg^{2+}$  binding than  $Ca^{2+}$ . In [24] it is argued that  $Mg^{2+}$  may bind covalently with AA, but by analogy with the  $Cd^{2+}$  case, we should expect an enhanced value for the binding constant as compared with  $Ca^{2+}$ . It is well known that  $Mg^{2+}$  has a very stable hydration sheath [26] and we suggest that  $Mg^{2+}$  binds electrostatically to oxygen retaining its hydration sheath (with a hydrated radius  $r_+ = 4.3 \text{ \AA}$  [26]). When the hydrated radius is used in eq. (8) (see table I), the calculated association constant is consistent with the experimental values. For  $Na^+$  ions we find no binding ( $pK < -2.5$ ). In general, we infer that the small lattice constant of AA results in a reduction of the binding constants by an order of magnitude or more from those obtained by eq. (8). This is in agreement with our own reflectivity data for  $Cs^+$  ions ( $r_+ = 1.7 \text{ \AA}$ ) next to phosphate groups [27]  $a_L = 6.8 \text{ \AA}$ . We also analyzed older experimental data [13] and found complete consistency with the results. We were not able to find similar data for trivalent ions.

*Conclusions.* – In this paper we have identified two correlation regimes, namely the TC and LC (fig. 1). The TC regime results in electrostatic binding to the interface, for which the association constants are computed by generalizing the Bjerrum theory [15]. Our approach accounts for ion specificity (see table I) by including the finite size of the ions and the nature of the head group charge through its size and from its  $pK_a$  value, which accounts for proton transfer and release. We compared our theoretical calculations with different experimental results and found good agreement, see table II and fig. 4.

The theory presented differs from previous theories [3–6] in that these theories assume a smeared interfacial charge distribution, where TC is absent, and deal with the LC. A scenario for the LC would be, for example, when interfacial charges are buried a distance  $d > 0.35a_L$  inside the interface. Our approach differs from previous theories on charge modulations [7, 8] in that it incorporates binding by Bjerrum pairing into LPB. For slightly charged modulated interfaces (defined by a small contact value potential relative to  $k_B T$ ) at low monovalent salt concentrations PB including modulations [9, 10] still applies.

In some situations (defined by amphiphile geometry and valence) we speculate that ions may penetrate inside the head group in a staggered configuration shown in fig. 2, forming a “molten salt” state consisting of the charged head groups and the mobile ions. This “molten

salt” state has a Madelung energy (given by the limit  $z \rightarrow 0$  in the corresponding fig. 2), and may lead to charge reversal. For moderate salt concentrations (defined by a Debye length smaller than  $a_L$ , the typical separation of charged interfacial groups), charge reversal of the interface by binding is also possible. Charge reversal has been experimentally observed in both membranes [12] and monolayers [28]. We have not discussed in any detail geometries other than the plane. We expect our arguments on Bjerrum induced correlation binding to apply for other geometries, such as cylinders, where equal charge attraction follows from binding [29].

It is imperative to compare theoretical ion distributions to experimental distributions that include points distant from the interface. Only recently, however, with the use of anomalous X-ray reflectivity techniques, are ion distributions becoming available [27, 28]. We hope to provide more detailed comparisons with those experimental results in the near future.

\* \* \*

The work of AT has been supported by NSF grant DMR-0426597. The work at the Ames Laboratory is supported by the DOE, office of Basic Energy Sciences under contract No. W-7405-ENG-82.

## REFERENCES

- [1] BOROUDJERDI H. *et al.*, *Phys. Rep.*, **416** (2005) 129.
- [2] GROSBERG A. YU., NGUYEN T. T. and SHKLOVSKII B. I., *Rev. Mod. Phys.*, **74** (2002) 329.
- [3] SHKLOVSKII B. I., *Phys. Rev. E*, **60** (1999) 5802.
- [4] MOREIRA A. G. and NETZ R., *Europhys. Lett.*, **52** (2001) 705.
- [5] BURAK Y., ANDELMAN D. and ORLAND H., *Phys. Rev. E*, **70** (2004) 016102.
- [6] SANTANGELO C., arXiv:cond-mat 0509007 (2005).
- [7] MOREIRA A. G. and NETZ R. R., *Europhys. Lett.*, **57** (2002) 911.
- [8] HENLE M. L., SANTANGELO C. D., PATEL D. M. and PINCUS P., *Europhys. Lett.*, **66** (2004) 286.
- [9] LUKATSKY D. B. and SAFRAN S. A., *Europhys. Lett.*, **60** (2002) 629.
- [10] TRAVESSET A., *Eur. Phys. J. E*, **17** (2005) 435.
- [11] GRAHAME D. C., *Chem. Rev.*, **1** (1947) 103.
- [12] MCLAUGHLIN S., *Annu. Rev. Biophys. Chem.*, **18** (1989) 113.
- [13] BLOCH J. M. and YUN W., *Phys. Rev. A*, **41** (1990) 844.
- [14] BOWICK M. *et al.*, *Phys. Rev. B*, **73** (2006) 024115.
- [15] ROBINSON R. A. and STOKES R. H., *Electrolyte Solutions* (Dover Publ., Mineola, NY) 1959.
- [16] PETRUCCI S., *Ionic Interactions* (Academic Press, New York, NY) 1971.
- [17] LEVIN Y. and FISHER M., *Physica A*, **225** (1996) 164.
- [18] TRAVESSET A., *Phys. Rev. E*, **72** (2005) 36110.
- [19] HANSEN J. P. and McDONALD I. R., *Theory of Simple Liquids* (Academic Press, London) 2003.
- [20] MARTELL A. E. and SMITH R. M. (Editors), *Critical Stability Constants* (Plenum, New York) 1974.
- [21] MCLAUGHLIN S. and BROWN J., *J. Gen. Physiol.*, **77** (1981) 445.
- [22] HUSTER D., ARNOLD K. and GAWRISCH K., *Biophys. J.*, **78** (2000) 3011.
- [23] KJAER *et al.*, *J. Phys. Chem.*, **93** (1989) 3200.
- [24] LE CALVEZ *et al.*, *Langmuir*, **17** (2001) 670.
- [25] SIMON-KUTSCHER J., GERICKE A. and HUHNERFUSS H., *Langmuir*, **12** (1996) 1027.
- [26] ISRAELACHVILI J., *Intermolecular and Surface Forces* (Academic Press, London) 2000.
- [27] BU W., VAKNIN D. and TRAVESSET A., *Phys. Rev. E*, **72** (2005) 60501.
- [28] VAKNIN D., KRUGER P. and LOSCHE M., *Phys. Rev. Lett.*, **90** (2003) 178102.
- [29] ARENZON J. J., STILCK J. and LEVIN Y., *Eur. Phys. J. B*, **12** (1999) 79.